The effect of spectral shape on damping modification factors

Sebastián Miranda,[a), c)] M.EERI, Eduardo Miranda,[b)] M.EERI and Juan Carlos de la Llera,[a)] M.EERI

The main objective of this study is to investigate the effect of spectral shape on damping modification factors η used in equivalent static and response spectrum analyses of structures with damping ratios that are different from 5% critical damping. Record-to-record variability of η is also evaluated through a statistical analysis of 5,270 ground motions records from 1,137 interface earthquakes recorded in Chile. The effect of spectral shape is studied by using recently developed spectral shape metrics *SaRatio* and epsilon (ε) and evaluating their use as possible predictors for η. Similarly to previous investigations, this paper also examines the effect of oscillator period, earthquake magnitude and duration for different levels of damping ratio. Results suggest that *SaRatio* is an effective predictor of η, particularly for highly damped structures. On the other hand, results also indicate that for rock and firm sites, earthquake faulting mechanism and site class do not have a significant influence on η. A simple period-independent regression model for η as a function of *SaRatio* and damping ratio is proposed. A comparison between median η from this study and those in current Chilean seismic codes shows that code factors are unconservative.

INTRODUCTION

Seismic design procedures require an intensity measure (IM), typically a spectral ordinate at a given vibration period S_a (T_1), taken from a pseudo-acceleration design spectrum or a ground motion prediction model (GMPM). In most cases, both approaches consider 5% damped spectral ordinates. However, there are several situations in which one is interested in estimating response spectrum ordinates for damping ratios higher than 5% (for example, in

[a)] National Research Center for Integrated Natural Disaster Management, CONICYT/FONDAP/15110017, Faculty of Engineering, Pontificia Universidad Catolica de Chile, Chile
[b)] John A. Blume Earthquake Engineering Center, Department of Civil and Environmental Engineering, Stanford University, Stanford, CA 94305-4020, U.S.A.
[c)] School of Engineering, Universidad del Desarrollo, Chile

structures with seismic isolation or with energy dissipation devices) or damping ratios smaller than 5% (for instance in high-rise buildings).

When systems with damping ratios different from 5% are under analysis, two approaches are typically considered: (1) using a GMPM specially developed for the desired damping ratio or; (2) scaling 5% damped ordinates by using damping modification factors η. The former approach has a significant limitation as there are only a few GMPMs that have been developed for damping ratios other than 5% and the few that are available have only been developed for specific seismically active regions. Furthermore, probabilistic seismic hazard analysis is typically only available for 5% spectral ordinates. That is why the latter approach is more frequently used, and it is currently implemented in most seismic design codes (e.g., ASCE/SEI 7-16 and NCh2745). This research is focused on damping modification factors η.

Damping modification factor η is defined as the ratio of the peak displacement of a linear SDOF with oscillator period T and damping ratio ξ to the peak displacement of a linear SDOF with the same oscillator period T and damping ratio 5%, as shown in the following expression:

$$\eta(T,\xi) = \frac{S_d(T,\xi)}{S_d(T,\xi = 5\%)} = \frac{A(T,\xi)}{A(T,\xi = 5\%)}$$

where

$$S_d(T,\xi) \equiv |u(t)|_{max}$$

and $u(t)$ is the displacement of the oscillator under analysis. $A(T,\xi)$ is the pseudo-acceleration spectral ordinate given by

$$A(T,\xi) \equiv {\omega_n}^2 S_d(T,\xi)$$

where ω_n is the circular frequency of vibration of the system.

The effects of viscous damping on the seismic response of linear SDOF systems have been studied since almost half a century when Newmark and Hall (1982) conducted their pioneer study. Since then, many models have been proposed to estimate η as a function of: (1) oscillator parameters, namely period of vibration T and damping ratio ξ; (2) earthquake magnitude and/or duration and distance to the source; and (3) site class. Lin et al. (2005) compared most relevant models to that date against mean damping modification factors computed with 216 ground motion records from firm sites in California.

Although most authors agree that η depends strongly on oscillator damping ratio and period of vibration, this period-dependence is currently neglected in most seismic design codes. Earthquake duration also affects η. In general, as duration increases, the effect of damping on the peak displacement becomes more pronounced.

Bommer and Mendis (2005) studied several GMPMs developed for damping ratios different from 5% and concluded that η is strongly dependent on earthquake magnitude and source-to-site distance. Cameron and Green (2007) performed a statistical analysis on 1,268 ground motion records finding that oscillator damping ratio and period of vibration, earthquake magnitude, and site class should be considered as predictors for η when the damping ratio is equal or higher than 2%. Also, they included source-to-site distance as a predictor for η when the damping ratio is equal to 1%. Moreover, several authors, including Boomer and Mendis (2005), Lin and Chang (2004), and Daneshvar et al. (2016) concluded that for rock and firm sites, site class does not have a significant influence on damping modification factors.

Stafford et al. (2008) developed a comprehensive study on damping modification factors considering different measures of duration but their recommendations were period independent. Rezaeian et al. (2012) developed a damping modification factor prediction model considering 2,250 horizontal ground motion records with rupture distances smaller than 50 km. They found a significant influence of earthquake duration on η. However, they noted that since earthquake duration is not explicitly considered when defining a seismic design scenario, they included the effect of duration indirectly through the use of magnitude as a predictor in their model given the strong positive correlation between duration and magnitude. Source-to-site distance, damping ratio, and oscillator period were also considered in their study as predictors for η. Bradley (2015) studied how some source-specific and site-specific effects influence the period-dependence of the damping modification factors η using ground motion records in New Zealand.

More recently, Daneshvar et al. (2016) performed a study of damping modification factors using ground motion records associated with the seismic hazard in southwestern British Columbia, Canada. This work differs from previous studies in the sense that it included the earthquake faulting mechanism as a predictor to estimate η. The inclusion of the type of seismic source was motivated by the fact that the seismic hazard in British Columbia includes shallow

crustal, deep inslab, and interface subduction earthquakes. They concluded that the earthquake faulting mechanism influences the damping modification factors η.

The main objectives of this research are: (1) to study the influence of magnitude, duration and site class on damping modification factors η computed from ground motions recorded during subduction earthquakes in Chile; (2) to investigate if there are any systematic differences in η computed from ground motions recorded in interplate or intraplate subduction earthquakes; (3) to study the influence of spectral shape on η; (4) to investigate the performance of two recently-proposed spectral shape proxy parameters as predictors of η; (5) to propose a simple period-independent model to estimate η as a function of *SaRatio* and damping ratio; and (6) to compare computed median η values to damping modification factors B_D and B_M specified in the current Chilean Code NCh2745 for seismic isolation.

GROUND MOTION DATABASE

The ground motion set used in this study consisted of 5,270 ground motion time histories recorded during 1,137 seismic events that occurred in Chile between 1985 and 2015. The seismic database used in this work was provided by the project SIBER-RISK (SIBER-RISK 2019). This database includes 1,004 interface events and 133 intraplate (inslab) events, resulting in 4,126 and 1,144 ground motions records, respectively.

Only events with magnitudes greater or equal than 5.0 were considered. The database includes several large-magnitude interface events that have taken place in Chile in recent years, including the 2010 M_w 8.8 Maule, 2014 M_w 8.2 Iquique, and 2015 M_w 8.4 Illapel earthquakes.

Site classes at the recording stations were classified using ASCE/SEI 7-16 (ASCE 2017) criteria based on the average shear wave velocity in the upper 30 meters of the site profile, V_{s30}. The database considers 68 records in site class A, 1,122 records in site class B, 3,014 records in site class C, and 1,066 records in site class D.

Figure 1 shows the magnitude versus source-to-site distance distribution (using R_{rup}, the minimum distance between the site and the rupture plane) for the ground motion set used in this study. The mean magnitude and the mean source-to-site distance in the dataset are 5.8 and 136 km, respectively, and are indicated by a red circle in Figure 1. Recorded peak ground accelerations in the dataset range from 0.01 g to 0.98 g.

While the arbitrary horizontal component approach is frequently used for engineering purposes, other horizontal component definitions as RotDxx or RotIxx

(Boore 2010) are preferred when sensor orientation significantly influences the seismic characterization, e.g., ground motion records reflecting directivity effects. In this study, the damping modification factors were calculated for arbitrary horizontal components and RotI50 horizontal components, and results show that, for the Chilean dataset under analysis, the difference between both approaches is negligible, as it can be seen in Figure 4. Based on this fact, this study is developed using the arbitrary component approach.

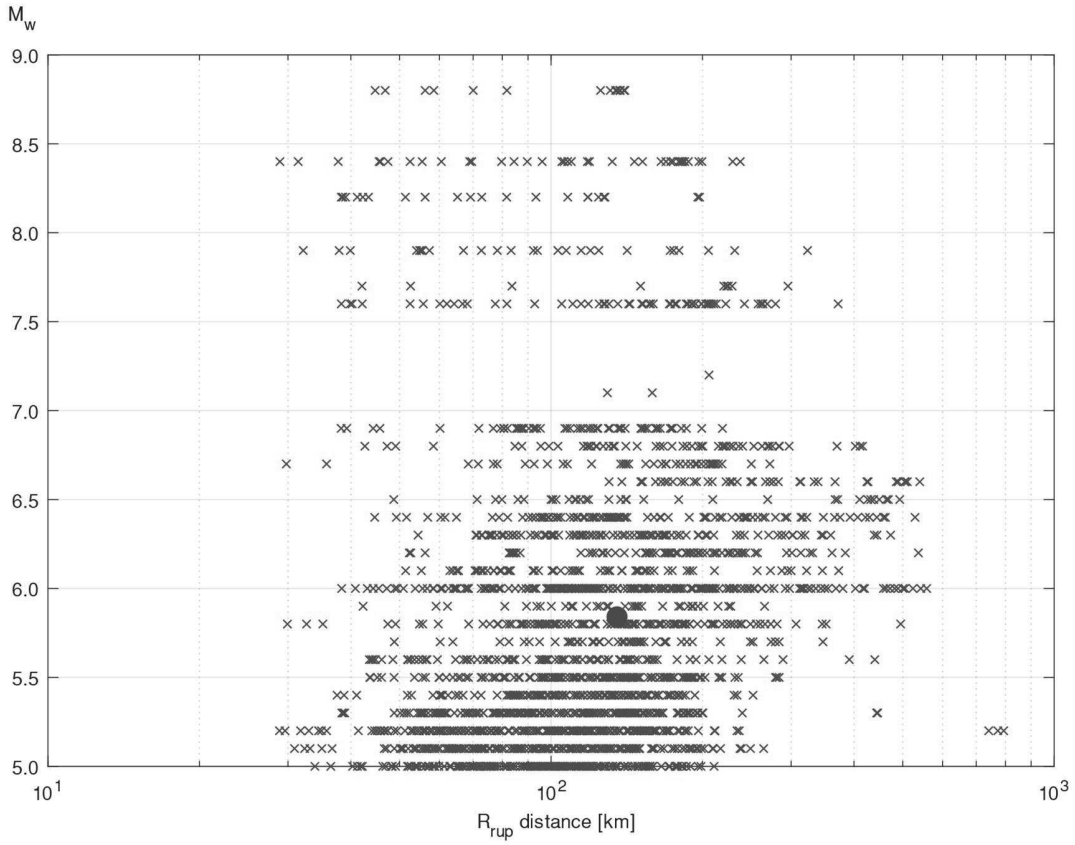

Figure 1. Magnitude versus source-to-site distance (minimum distance between source and site, R_{rup}) for the considered ground motion database.

For each recorded ground motion, two different significant durations were computed, namely D_{5-75} and D_{5-95} (Bommer and Martinez-Pereira 1999). Figure 2 shows that for the ground motions considered in this study, the correlation between duration and moment magnitude is quite similar for both duration parameters with coefficients of determination (R^2) of 0.22 for D_{5-75} and 0.23 for D_{5-95}, indicating no relevant difference between the use of one or the other. This is consistent with results by Stafford et al. (2008) that concluded that there was no significant difference between both duration measurements when used as a predictor to estimate η. Figure 3 shows the correlation between both duration measures and source-to-site

distance (R_{rup}). In this case, D_{5-75} shows a higher correlation with R_{rup} than D_{5-95}, with coefficients of determination (R^2) 0.32 and 0.16, respectively.

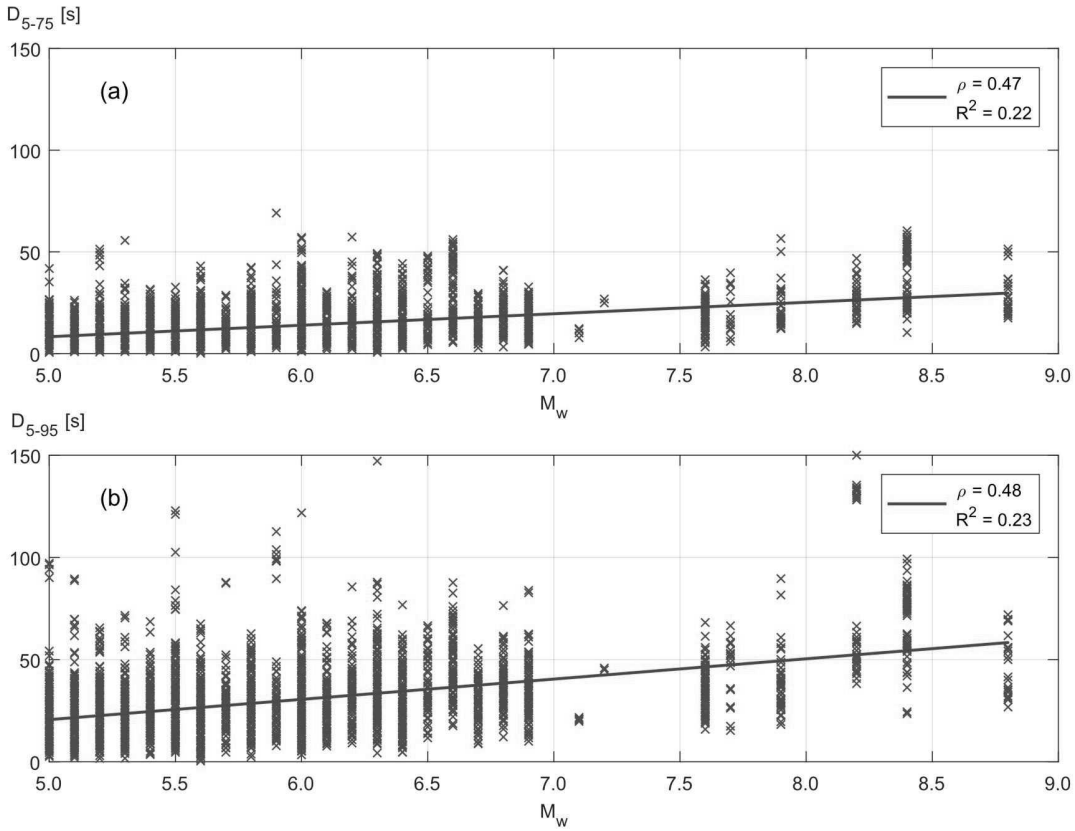

Figure 2. Variability of record duration as a function of magnitude; (a) D_{5-75} versus M_{w}, and (b) D_{5-95} versus M_{w}.

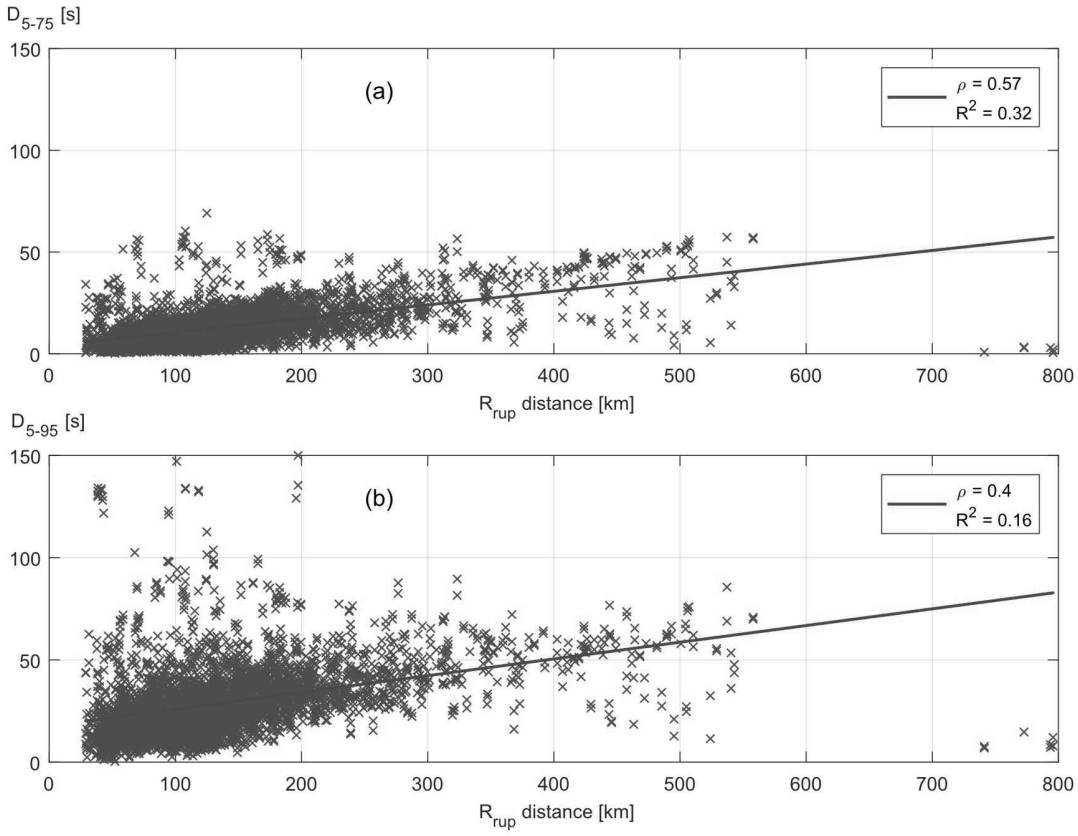

Figure 3. Variability of record duration as a function of source-to-site distance (minimum distance between source and site, R_{rup}); (a) D_{5-75} versus R_{rup}, and (b) D_{5-95} versus R_{rup}.

DAMPING MODIFICATION FACTORS

To assess the relationship between η and different predictors, damping modification factors were computed using the ground motion database described above for damping ratios of $\xi = 0.5\%, 1\%, 2\%, 3\%, 4\%, 5\%, 8\%, 10\%, 12\%, 15\%, 18\%, 20\%, 25\%, 30\%,$ and 50% and a range of oscillator periods between 0.05 s and 6 s, with a period interval of 0.01 s.

Figure 4 shows median η values as a function of oscillator period for the complete ground motion dataset and selected damping ratios $\xi = 1\%, 2\%, 3\%, 10\%, 20\%,$ and 30%. Median values were calculated for arbitrary horizontal components and RotI50 horizontal components, and results are shown in blue solid and red dashed lines, respectively. The shaded area represents the η-values between the 16th and 84th percentiles, showing that dispersion around the median significantly increases as the damping ratios depart from 5%.

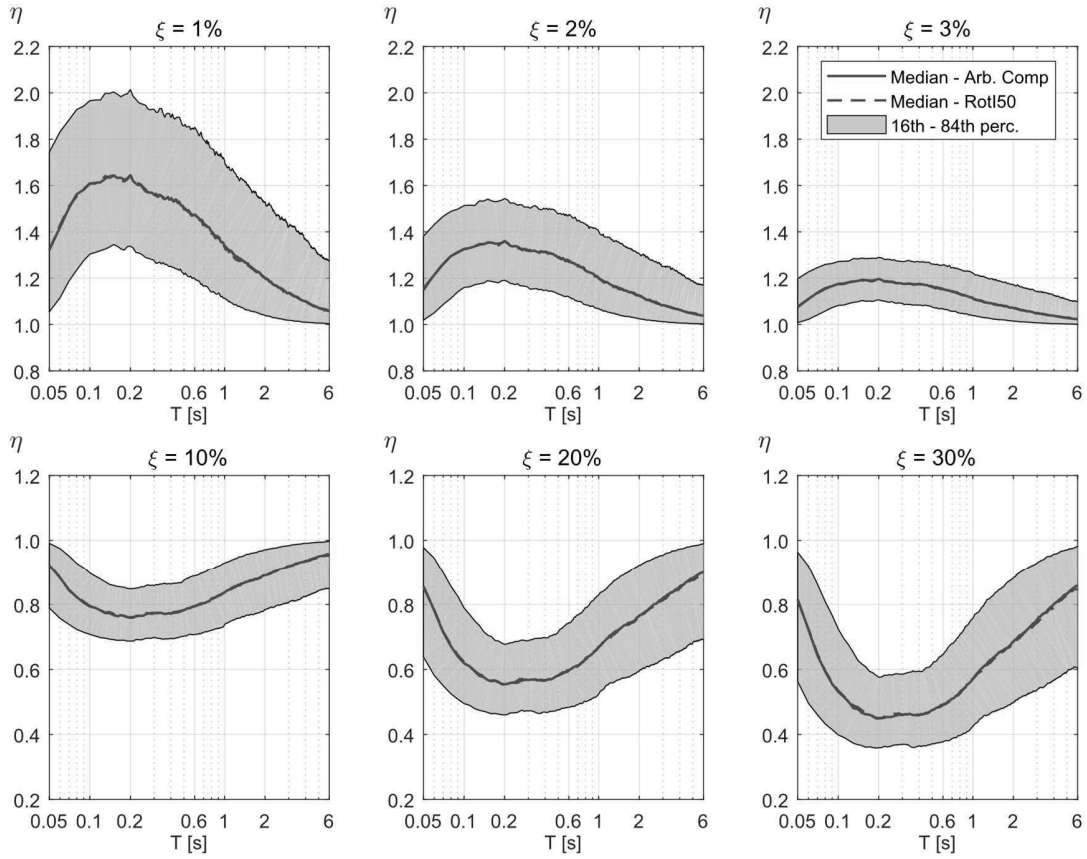

Figure 4. Effect of damping ratio and oscillator period on median η values, considering arbitrary horizontal components and RotI50 horizontal components, in blue solid and red dashed lines, respectively. The shaded area represents values between the 16th and 84th percentiles of η.

As it has been extensively stated in the literature (Bommer and Mendis 2005, Rezaeian et al. 2012) earthquake magnitude and duration have a relevant effect on damping modification factors η. Higher magnitude earthquakes tend to have longer duration, leading to more significant response reductions in highly damped systems, and more significant response increases in low damping systems. Figure 5 shows the calculated median of η as a function of oscillator period when the ground motion dataset is binned by magnitude. Considered magnitude intervals were [5.0 - 6.0), [6.0 - 7.0), [7.0 - 8.0), and above 8.0, with 3202, 1698, 218, and 152 ground motion records, respectively. **To isolate the effect of magnitude and to neutralize any relevant site effect, damping modification factors were normalized to a constant V_{s30} value of 760 m/s, by implementing the damping modification factor prediction model developed by Akkar et al. (2014) for assessment of the normalizing factor. Median η values calculated without normalization and median η values normalized to $V_{s30} = 760\ m/s$ are shown in solid and dashed lines, respectively. It is**

observed that site correction has a mild influence on median values, especially in oscillators with vibration periods higher than 4.0 seconds and high damping ratio.

Results show a strong influence of earthquake magnitude on η. For example, an oscillator with a vibration period of 3.0 s and 20% damping ratio shows median η values of 0.89 and 0.61, for earthquakes in the [5.0 - 6.0) and the above 8.0 intervals, respectively, indicating an additional reduction in spectral ordinates of 31% in the higher magnitude scenario. Larger jaggedness in the curves corresponding to the two larger magnitudes bins, particularly for damping ratios of 1% and 2%, are the result of the smaller number of ground motions in these bins.

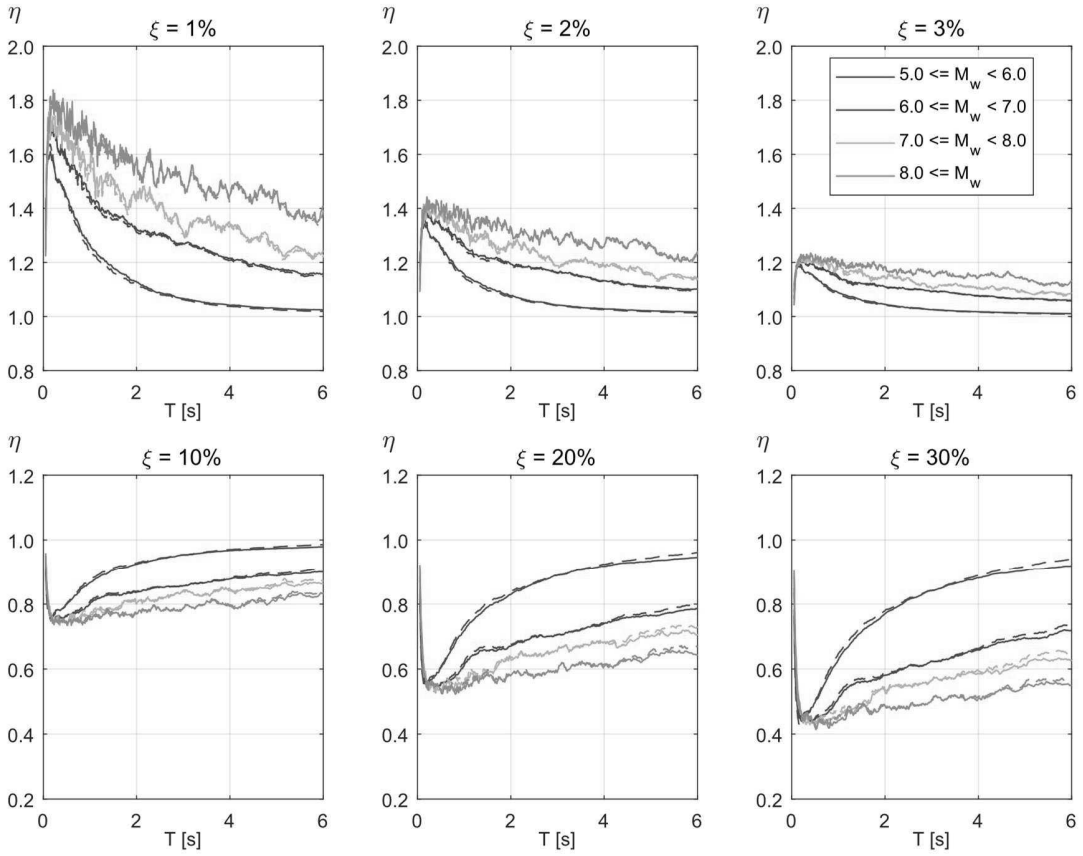

Figure 5. Effect of magnitude on median η values, calculated without site effect normalization and calculated with site effect normalization, in solid and dashed lines, respectively.

To investigate if differences in η calculated in this study and those calculated by Lin and Chang (2004) are due to differences in the earthquake faulting mechanism or due to differences in magnitudes, two subsets of the Chilean database were considered by selecting records

associated with: (i) events of minimum magnitude 5.7 (to achieve a mean magnitude similar to that in Lin and Chang, 2004); and (ii) events of magnitude 8.0 or above.

Figure 6 compares median damping modification factors η computed in this study (for two subsets with minimum magnitudes of 5.7 and 8.0) with: (i) those currently specified in the Chilean code for seismically isolated structures NCh2745; (ii) those proposed by Lin and Chang (2004); and (iii) those currently specified in ASCE/SEI 7-16. Results show that median η values from this study, when the 5.7 minimum magnitude subset and damping levels higher than 5% are considered, are much closer to the equation proposed by Lin and Chang (2004) for crustal earthquakes in the United States than to the equations used in the Chilean code NCh2745. On the other hand, results for the 8.0 minimum magnitude subset tend to be more consistent with the trends proposed by Chilean code NCh2745.

Results from Figure 6 also show that damping modification factors specified by the Chilean code NCh2745 (INN 2013) are unconservative in the complete period range when damping ratios higher than 5% are considered. For example, for a hypothetical case of an isolated building with an effective oscillator period of 3.0 s and an effective damping ratio of 20%, the 5% design spectral ordinate is reduced, according to the Chilean code procedure, by a factor of 0.52. However, the median value of η obtained for the 5.7 minimum magnitude ground motion subset is 0.70. In other words, the code is unconservative as the spectral ordinate is reduced 25% more than the median reduction computed from recorded ground motions.

Damping modification factors in the Chilean code were based on a set of records from the 1985 Chile earthquake (M_w 7.9) that were spectrally matched in the frequency domain to the NCh2745 design spectrum. Naeim and Lew (1995) found that frequency-domain spectrally-matched ground motions could include high levels of input energy spread in a wide band of periods, then the η factors obtained from these synthetic records tend to overestimate the reduction in the response. As stated by Hancock et al. (2006) this effect could be minimized by using an improved time-domain spectral matching approach that simultaneously matches spectra corresponding to different levels of damping. Consequently, it is recommended that new versions of the code define damping modification factors from time-domain spectrally matched records or from real earthquake records, like the ones presented in this study.

It should be noted that expressions in NCh2745 were never intended to be applied for structures with internal damping less than 5%, but if such expressions are used, for example in the design of high rise buildings whose damping ratios in the fundamental period are much smaller than 5%, they will lead to conservative results.

The Chilean code for earthquake-resistant design of industrial structures and facilities, NCh2369 (INN2003), considers a period-independent expression given by $\eta = (0.05/\xi)^{0.4}$. In this case, for the hypothetical case of a system with an effective damping ratio of 20%, a reduction factor of 0.57 is applied resulting also in an unconservative design.

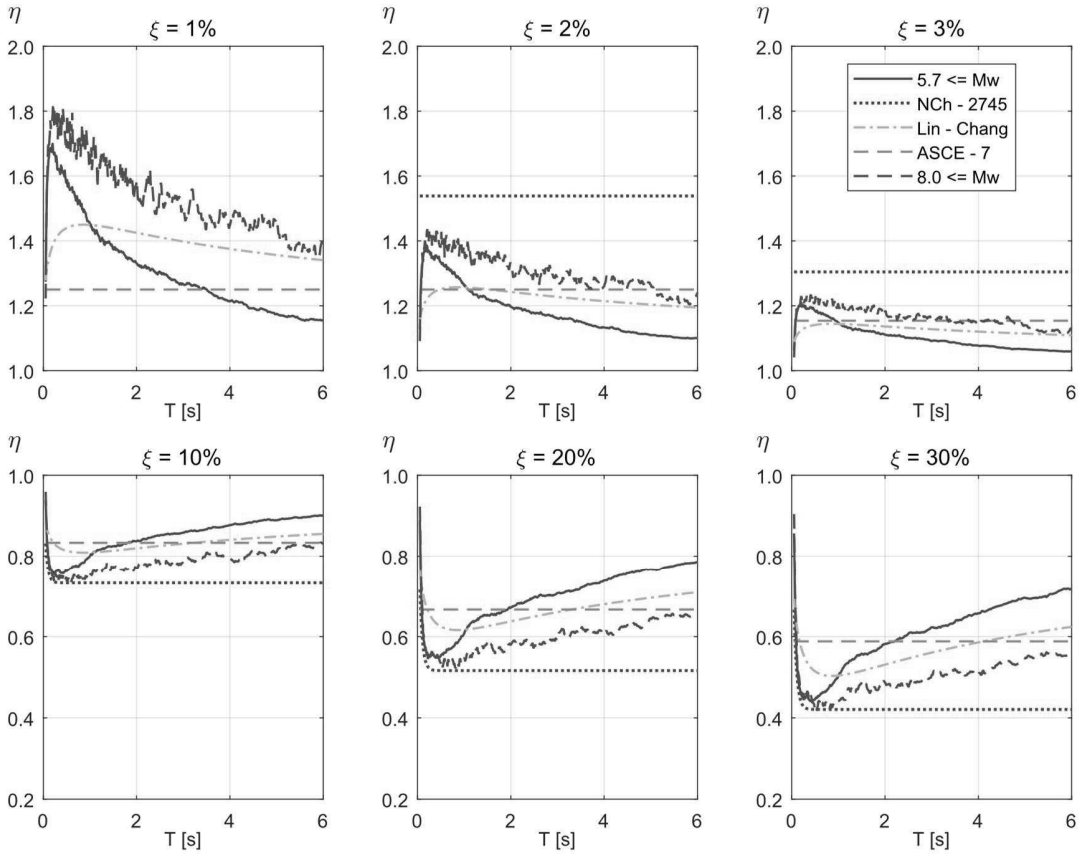

Figure 6. Damping modification factors: (i) median values calculated from a sub-set of Chilean ground motions with a minimum magnitude of 5.7; (ii) values currently specified in NCh 2745; (iii) values predicted by Lin and Chang (2004) model; (iv) values currently specified in ASCE/SEI 7-16; and (v) median values calculated from a sub-set of Chilean ground motions with a minimum magnitude of 8.0

Daneshvar et al. (2016) proposed damping modification factors that depend on the earthquake faulting mechanism, as the seismic hazard in British Columbia is affected by shallow crustal, deep inslab, and interface subduction earthquakes. The authors studied the

differences in frequency content in inslab and interface events, by using their mean period T_m (Rathje et al. 2004) concluding that inslab events have, on average, a lower mean period resulting in smaller damping modification factors η for short period structures. **However, it should be noted that, in their study, in addition to changes in the frequency content of ground motions recorded from inslab or interface events, there may be significant differences between their durations and magnitudes, that should also be considered when predicting η factors.**

To investigate the effect of seismic source on η, ground motions considered in this study were classified based on their faulting mechanism. Figure 7 shows the distribution of magnitudes and D_{5-95} durations for interface and inslab records. Interface events present higher magnitudes than their corresponding inslab events with mean magnitudes of 5.9 and 5.6, respectively. This difference in magnitudes in interface and inslab events was found to be statistically significant. This statistically significant difference in magnitudes in interface and inslab events was also found to occur when examining the magnitude of subduction events contained in the NGA-Sub project (Bozorgnia and Stewart 2020). However, for the ground motions in our database the mean D_{5-95} duration is 29 s for both source cases. Bommer and Mendis (2005) studied the effect of both magnitude and duration on η. They concluded that duration, which is strongly correlated to earthquake magnitude, has a relevant effect on η; therefore, it is important to evaluate the effect of the faulting mechanism separate from the effect of earthquake magnitude or duration.

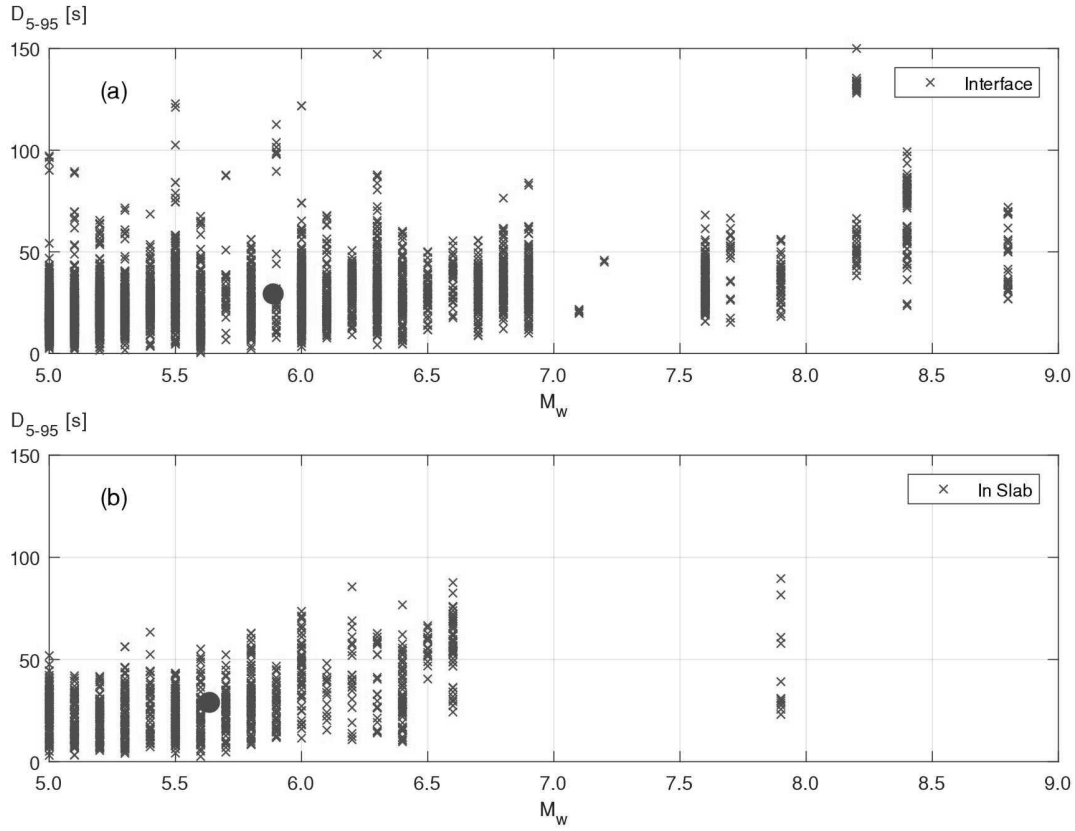

Figure 7. Duration D_{5-95} versus magnitude; (a) interface subduction events, and (b) inslab events.

To evaluate the effect of faulting mechanism, the median η values for two subsets of interface and inslab events with the same mean magnitude of 5.42 and the same mean D_{5-95} duration of 11.3 s are displayed in Figure 8. As shown in this figure, when events with similar magnitudes and durations are compared, there are no systematic differences between the median η values. Variability in η also does not seem to be significantly influenced by the type of source mechanism.

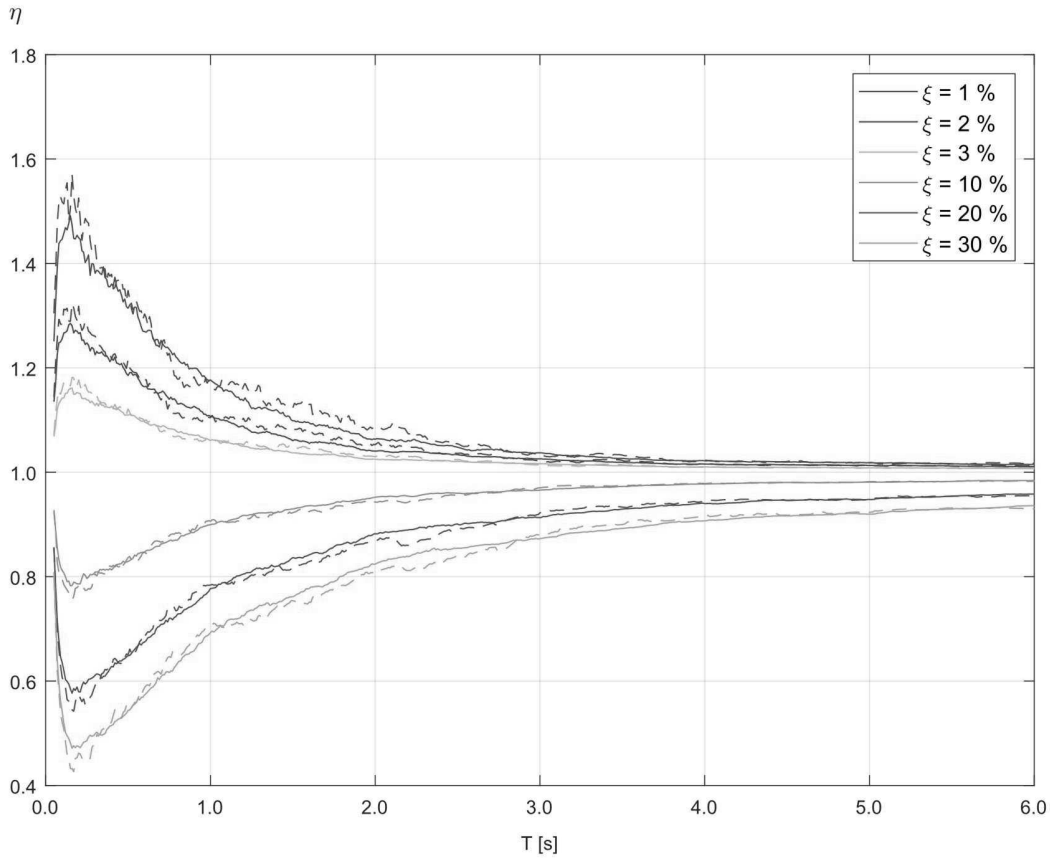

Figure 8. Median η values as a function of oscillator period for interface ground motion set and inslab ground motion set, in solid and dashed lines, respectively.

Lin and Chang (2004) performed a study on the site class effect on η. When considering rock and firm soils they concluded that site class produced differences smaller than 5% on mean η values. In this study, η factors were grouped as a function of site conditions at each recording station using the site classes defined in ASCE/SEI 7-16 according to the V_{s30} parameter. **To purely reflect the site class effect, damping modification factors were normalized to: i) a constant magnitude of 5.8, and ii) a rupture distance of 136 km, by implementing the damping modification factor prediction model developed by Akkar et al. (2014). These normalizing values were selected since they are the mean magnitude and the mean distance for the complete ground motion dataset.**

Figure 9 compares median normalized η factors for ground motions recorded at site classes A, B, C, and D. As shown in this figure, site class (for those site classes) does not have a significant effect on median η. There is a greater effect in site class D and higher damping ratios (equal or higher than 20%). The jaggedness shown in the curves corresponding to site class A is due to the significantly smaller number of ground motions recorded in this site class

(68) than for the other site classes (1122, 3014, and 1066 for site classes B, C, and D, respectively).

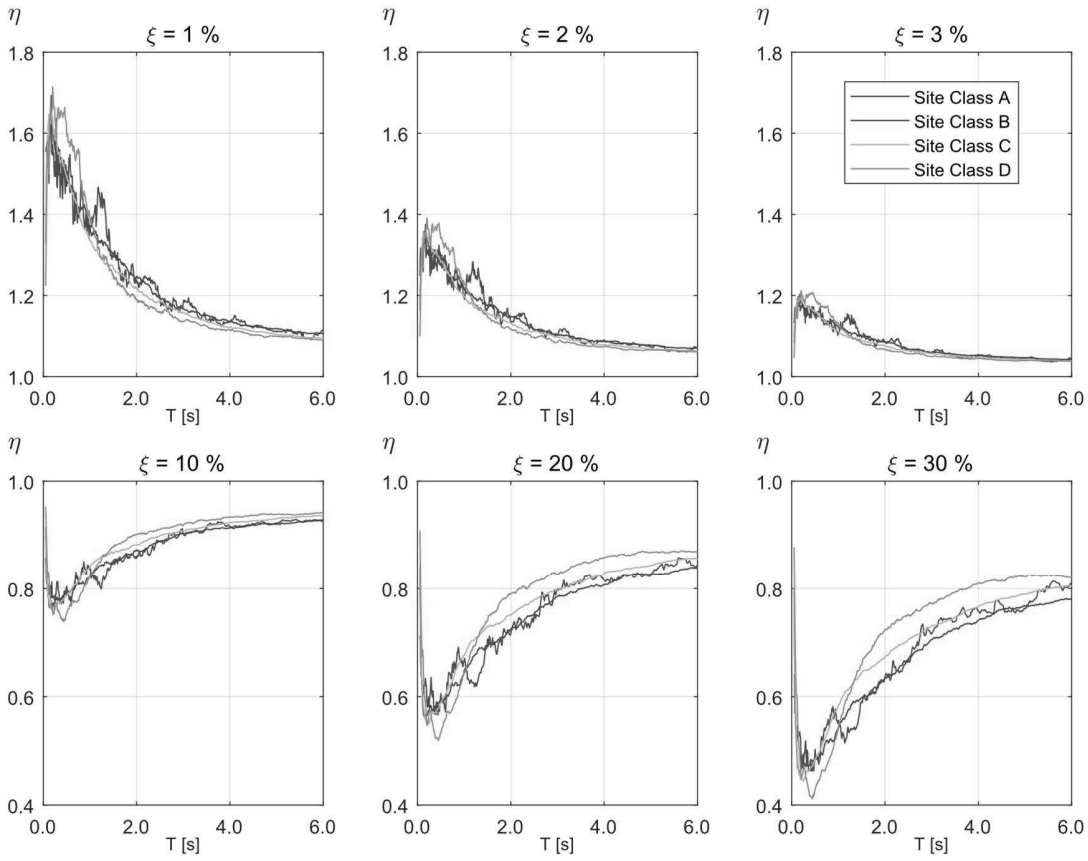

Figure 9. Effects of site class (following ASCE/SEI 7-16 classification) on median η values as a function of oscillator period.

SPECTRAL SHAPE METRICS

Consistent with previous studies, we found that η factors are primarily dependent on the damping ratio and the period of vibration of the oscillators. However, while most seismic design codes consider the damping ratio dependency, most specify period independent η factors. Another weakness of current design procedures is that earthquake magnitude or duration, are also not explicitly considered in the estimation of η, although their influence has been widely established in the literature (e.g., Bommer and Mendis 2005, Rezaeian et al. 2012) and also corroborated by the results of this work.

Recent studies have shown that in addition to causal parameters such as earthquake magnitude and source-to-site distance, spectral shape may have an important influence on the

seismic response of structures. To study the influence of spectral shape on η factors, two different spectral shape metrics were evaluated as possible predictors when estimating η.

The first approximate measure of spectral shape that was evaluated was epsilon (ε) which is defined as the number of logarithmic standard deviations that a given spectral ordinate is above or below the median value predicted by a GMPM and is evaluated by the following expression:

$$\varepsilon(T) \equiv \frac{ln\, Sa(T) - \mu_{LnSA}(M,R,T)_{GMPM}}{\sigma_{LnSA}(T)_{GMPM}}$$

where $ln\, Sa(T)$ is the natural logarithm of the spectral pseudo-acceleration ordinate at a given vibration period T, and $\mu_{LnSA}(M,R,T)_{GMPM}$ and $\sigma_{LnSA}(T)_{GMPM}$ are the values of the mean and the standard deviation of $ln\, Sa(T)$, respectively, as predicted by a representative GMPM, being all the defined quantities typically calculated for a 5% damping ratio. Epsilon (ε) depends on the GMPM selected for its evaluation, but Baker and Cornell (2006) concluded that its value does not show a strong dependency on the GMPM used in its calculation. Consequently, in this work epsilon (ε) values were calculated using the GMPM developed by Montalva et al. (2017) for the Chilean subduction zone given that the ground motion set used in our statistical study is quite similar to the set used for the development of their GMPM. **It should be noted that as Montalva GMPM predicts geomean spectral ordinates and this study considers arbitrary horizontal components, a correction factor, based on the results presented in Beyer and Bommer (2006), was considered when epsilon (ε) values were calculated.**

The second approximate measure of spectral shape is *SaRatio,* whose robustness as collapse predictor was analyzed by Eads et al. (2016). **It is defined as the 5% damping ratio spectral ordinate at the oscillator period of interest T_1, normalized by the geometric mean of the 5% damping ratio spectral ordinates over a period range, defined by two non-negative parameters a and b, and is evaluated with the expression:**

$$SaRatio = \frac{Sa(T_1, \xi = 5\,\%)}{Sa_{avg}([a \cdot T_1, b \cdot T_1])}$$

where

$$Sa_{avg}([a \cdot T_1, b \cdot T_1]) = \left(\prod_{i=1}^{N} Sa\,(T_i, \xi = 5\,\%) \right)^{\frac{1}{N}}$$

and

$$\boldsymbol{T_i = \left(a + \frac{(i-1)}{(N-1)}(b-a)\right) T_1}$$

N is the number of ordinates, typically equally spaced, considered in the average. In this study we used 100 equally spaced spectral ordinates.

For instance, Eads et al. (2016) found that for a wide range of buildings, the values of a and b that maximize the correlation between *SaRatio* and collapse intensity are 0.2 and 3.0, respectively. An optimal period range needs to be selected to maximize the correlation between *SaRatio* and η by selecting appropriate values for a and b factors. An extensive calculation was implemented herein for this purpose considering SDOF oscillators with vibration periods T = 0.25 s, 0.50 s, 0.75 s, 1.00 s, 1.25 s, 1.50 s, 1.75 s, 2.00 s, 2.25 s, 2.50 s, 2.75 s, and 3.00 s and damping ratios of ξ = 1%, 2%, 10%, and 20%, leading to a total of 48 cases. Parameters η and *SaRatio* were calculated for each ground motion record and the quality of a linear regression was evaluated through their coefficient of determination R^2, which was computed for each pair of a and b factors. Indeed, this procedure was repeated for all possible combinations of a and b, ranging from 0.02 to 0.98 and 1.04 to 4.00, respectively.

Figure 10 displays contour curves of equal R^2 for each a and b pair, considering SDOF systems with vibration periods T = 0.50 s, 1.50 s, and 3.00 s, and 2% and 20% critical damping ratio, showing that the maximum coefficient of determination R^2 between η and *SaRatio* is higher for highly damped systems and reaches a maximum value of 0.62 for an oscillator with $T_n = 3\ s$ and $\xi = 20\%$. On the other hand, systems with low damping, say 2%, show significantly smaller correlation and reach a maximum R^2 value of 0.30 for $T_n = 3\ s$ and $\xi = 2\%$.

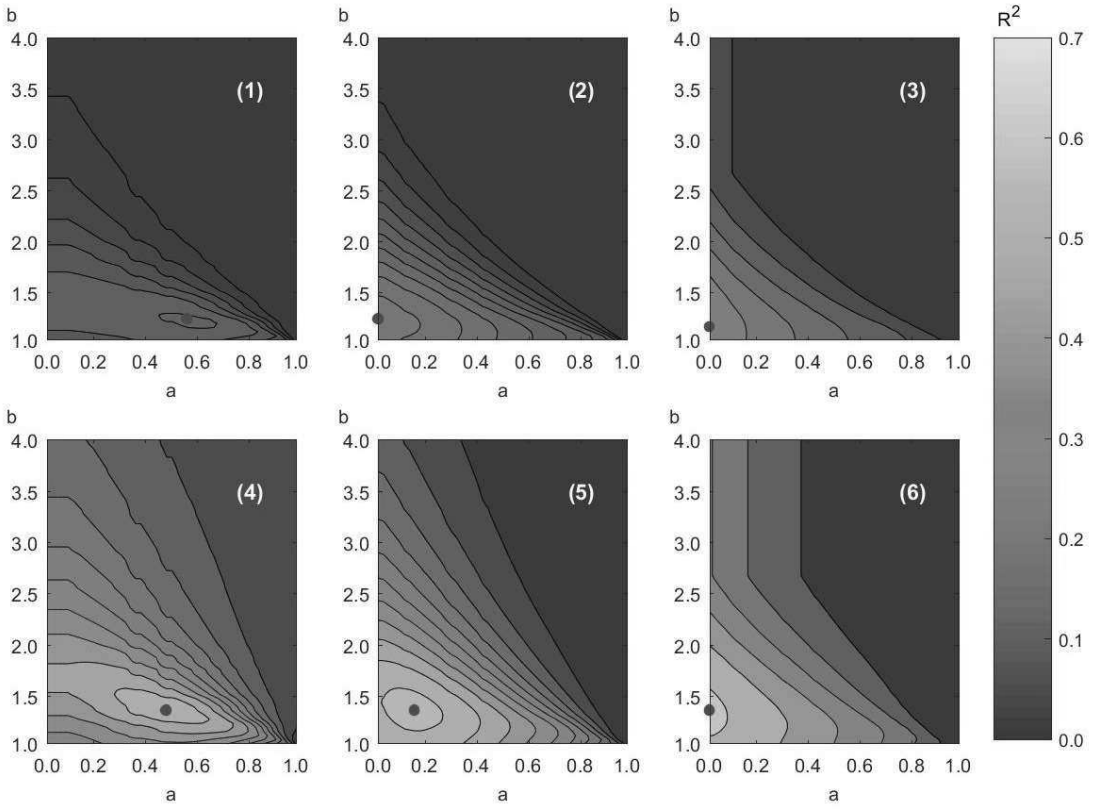

Figure 10. Contour curves of equal R^2 for η as a function of *SaRatio* for different a and b pairs: (1) $T = 0.5\ s$ and $\xi = 2\%$; (2) $T = 1.5\ s$ and $\xi = 2\%$; (3) $T = 3.0\ s$ and $\xi = 2\%$; (4) $T = 0.5\ s$ and $\xi = 20\%$; (5) $T = 1.5\ s$ and $\xi = 20\%$; and (6) $T = 3.0\ s$ and $\xi = 20\%$.

The optimal b factor, that is the one that maximizes the coefficient of determination R^2, varies with the oscillator period and the damping ratio, but it is typically between 1.1 and 1.4. There is, however, a small increment of b with increasing values of ξ. On the other hand, optimum values of a present more variability ranging from 0.02 (i.e., the complete spectral zone to the left of the vibration period of interest) to 0.8. In general, optimum values of a decrease as the oscillator period increases. This variability is summarized in Figure 11, which shows how optimal values of a and b vary as a function of vibration period and damping ratio.

Results of Figure 10 suggest that there is a significant correlation between η and *SaRatio,* especially in systems with high damping ratio and long vibration period (e.g., structures with seismic isolation or energy dissipators devices). However, as Figure 11 shows, the optimal values of a and b that maximize this correlation are period dependent, thus presenting an additional complexity when using *SaRatio* as a predictor.

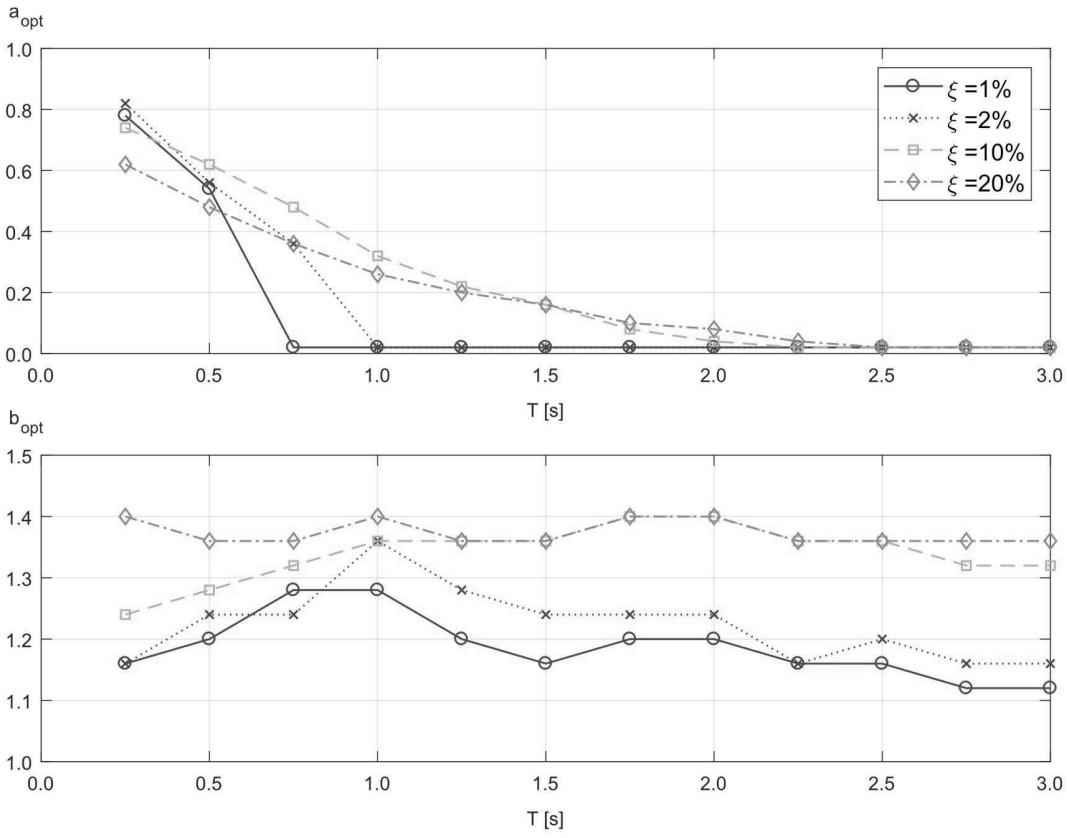

Figure 11. *a* and *b* factor optimal values as a function of vibration period for different damping ratios.

To propose a simplification in the *SaRatio* calculation procedure, an interval of $[0.2 \cdot T_1, 1.3 \cdot T_1]$ independent of vibration period and damping ratio was used to evaluate the correlation between η and *SaRatio*. Figure 12 compares the values of R^2 calculated when using optimal values of *a* and *b*, depending on the oscillator parameters when computing *SaRatio*, and when using *a* and *b* fixed to 0.2 and 1.3, respectively. As shown in this figure, there is a significant difference between the R^2 values computed using optimal versus constant *a* and *b* factors for short period oscillators with high-damping ratios. However, in structures with low damping ratios, regardless of vibration period, and in structures with high damping ratios and vibration periods longer than T = 1.0 s the difference is relatively small (less than 10% difference from the optimal R^2 value). Hence, this constant interval appears to provide relatively good results leading to a more straightforward procedure, especially in structures equipped with seismic isolation whose effective periods tend to be long. Therefore, this approach will be used in the remaining sections of this document.

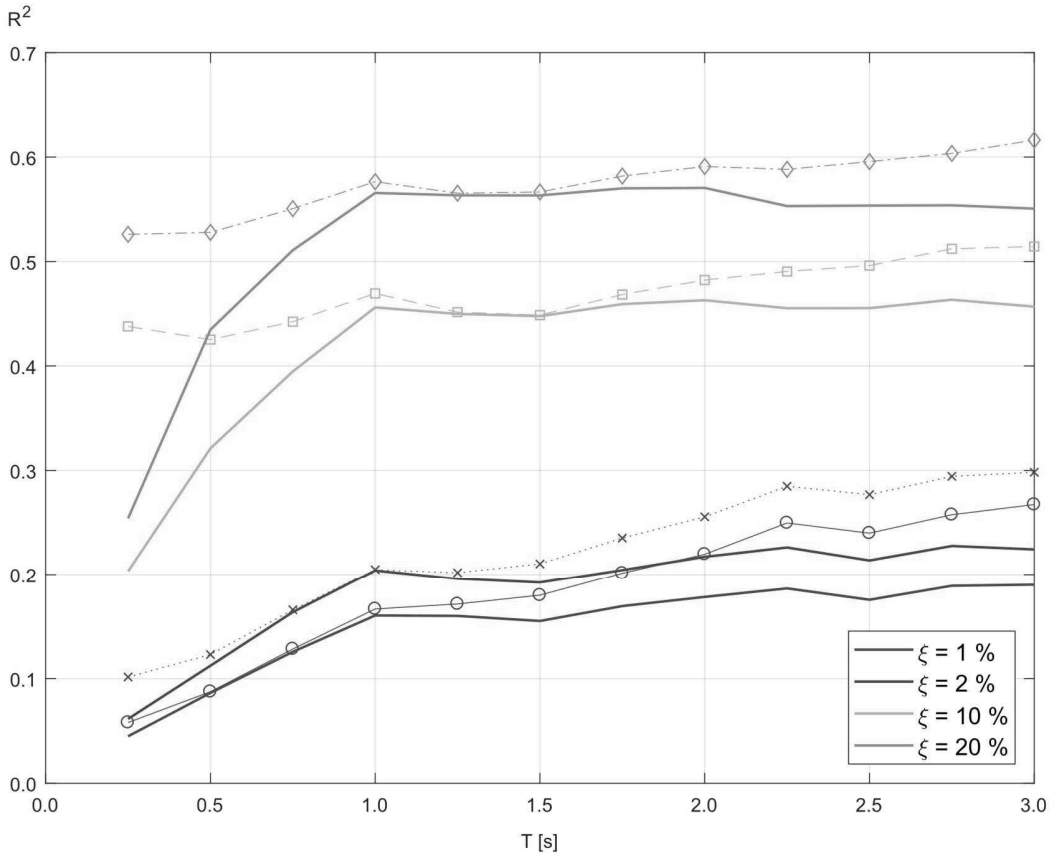

Figure 12. R^2 values measuring the correlation between η and *SaRatio* as a function of vibration period and damping ratio for two different methodologies to compute *SaRatio*: (1) considering optimal values of a and b factors; and (2) considering constant values of a and b factors, displayed with markers and solid lines, respectively.

EVALUATION OF POSSIBLE PREDICTORS

Having already defined the period range for *SaRatio* calculation, the capabilities of different parameters were assessed as possible predictors of damping modification factors η. **Figure 13 shows scatter plots of η, calculated for an SDOF oscillator with T = 3.0 s and $\xi = 20\%$, as a function of magnitude, significant duration D_{5-95}, epsilon (ε), and *SaRatio* for the complete dataset of ground motion records. It should be explicitly stated here that spectral shape metrics epsilon (ε) and *SaRatio* were calculated considering 5% damping ratio, as their capabilities as spectral shape proxies are not strongly dependent on the damping ratio considered in their calculation.**

A regression curve (linear or exponential, the one that fits best) is drawn through the data. As shown in Figure 13, *SaRatio* performs significantly better as a predictor than the other three parameters showing a coefficient of determination R^2 of 0.56 with an exponential model,

followed by earthquake magnitude with an R^2 value of 0.33, duration D_{5-95} with an R^2 value of 0.15, and finally epsilon showing practically no correlation with η. The same conclusion can be drawn when the Akaike information criterion (AIC) was implemented to compare the relative quality of the models. Due to space limitations, only results for this oscillator period and damping ratio are shown, but this trend was observed in all the oscillators with damping ratios higher than 10%. In the electronic supplement of this manuscript, plots for different periods of vibration and damping ratios are included.

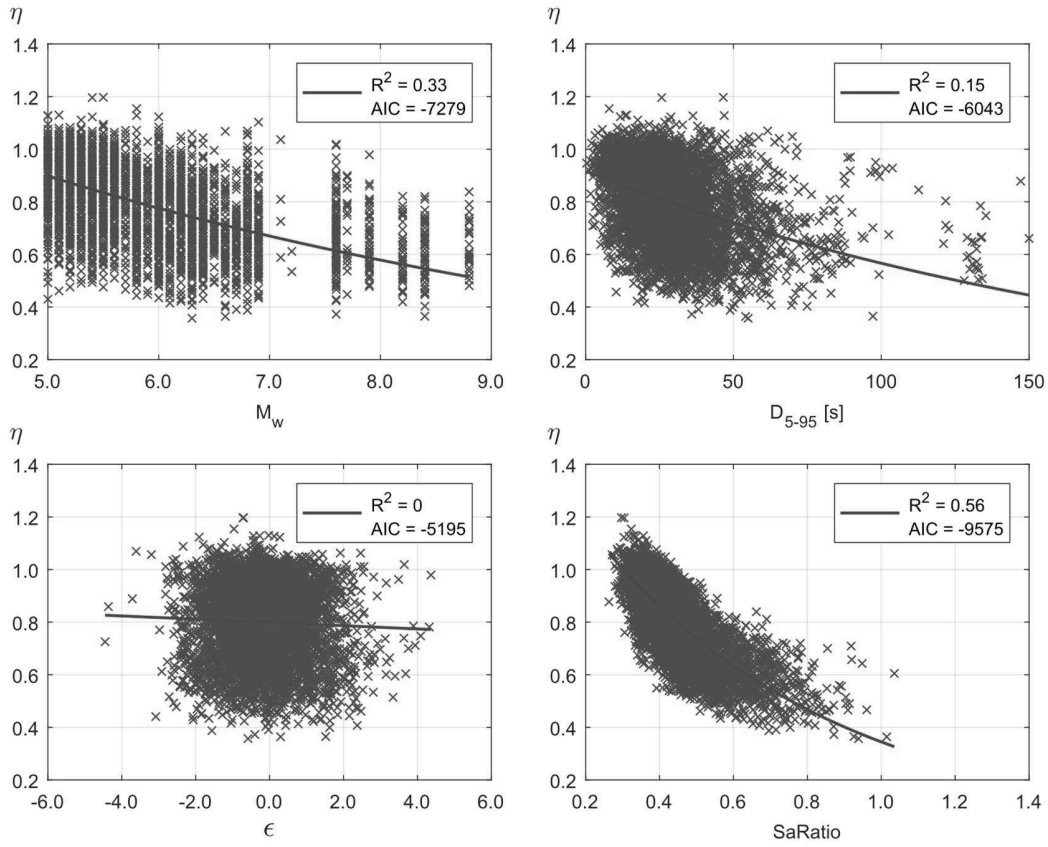

Figure 13. η values as a function of earthquake magnitude, duration D_{5-95}, epsilon (ε), and *SaRatio* for the complete ground motion set and an SDOF oscillator with T=3.0 s and $\xi = 20\%$.

Coefficients of determination R^2 for regression of η as a function of *SaRatio* are presented for different vibration periods and damping ratios in the first subplot of Figure 14. R^2 values higher than 0.4 are obtained for SDOF systems with vibration periods longer than 0.5 s and damping ratios higher than 10%; this correlation metric increases rapidly as the damping ratio increases. For example, an SDOF with T = 1.0 s and $\xi = 50\%$ has a coefficient of determination of 0.72, indicating that most of the record-to-record variation in damping modification factors η is due to changes in *SaRatio.* As shown in the figure, for systems with

damping ratios lower than 10% correlation decreases rapidly regardless of the oscillator period considered.

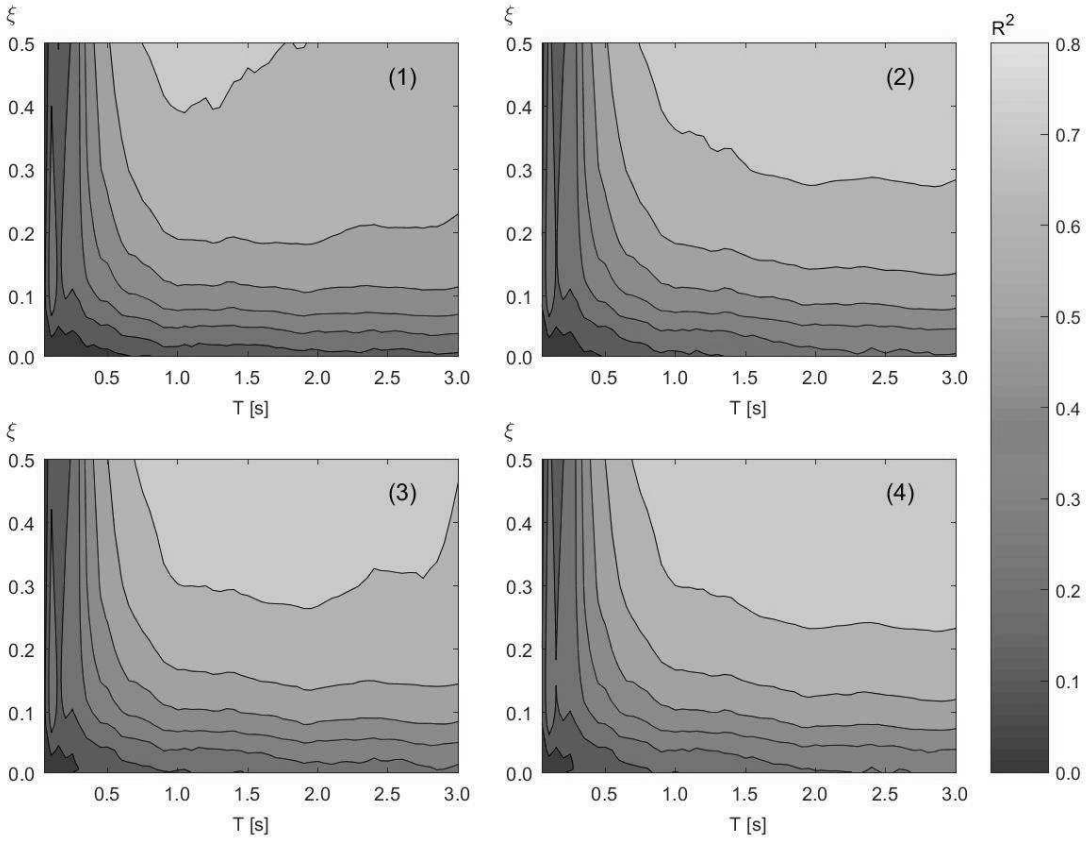

Figure 14. Contour curves of equal R^2 for different combinations of oscillator periods and damping ratios when using different predictors: a) *SaRatio*; b) *SaRatio* and earthquake magnitude; c) *SaRatio* and duration D_{5-95}; and d) *SaRatio*, earthquake magnitude, and duration D_{5-95}.

To evaluate if this exponential model could be improved by including more than one predictor, the following functional forms were also evaluated:

$$\eta = a_1 \cdot \exp\left(b_1 \cdot SaRatio + c_1 \cdot M_w\right)$$

$$\eta = a_2 \cdot \exp(b_2 \cdot SaRatio + c_2 \cdot D_{5-95})$$

$$\eta = a_3 \cdot \exp(b_3 \cdot SaRatio + c_3 \cdot M_w + d_3 \cdot D_{5-95})$$

where a_i, b_i, c_i and d_i are constants obtained through nonlinear regression to minimize differences between the observed and estimated values of η.

Contour plots for these models are also displayed in Figure 14 on plots b), c), and d), respectively. A mild improvement is observed, when including additional predictors in addition to *SaRatio*, especially for long period oscillators and damping ratios higher than 30%. Figure

15 presents coefficients of determination R^2 for the four models considered in this study (based on *SaRatio* and additional predictors M_w and D_{5-95}) and those of: (1) a model with source-to-site distance R_{rup} as the only predictor; (2) a model with earthquake magnitude M_w as the only predictor; and (3) a model with earthquake magnitude M_w and source-to-site distance R_{rup} as predictors. The comparison was performed at damping ratios of 2%, 10%, and 20%, and a range of periods of vibration between T = 0.05 s and 3.00 s. Since the correlation level is relatively low for periods of vibration less than T = 1.0 s and a damping ratio of 2%, there are no significant differences between the different models in this period range. However, as the oscillator period and the damping ratio increase, models using only *SaRatio* or *SaRatio* combined with additional parameters as predictors, significantly improve their R^2. Even though additional improvement can be achieved by using more complex models, herein only the model predicting η as a function of *SaRatio* (in addition to T and ξ) will be further pursued.

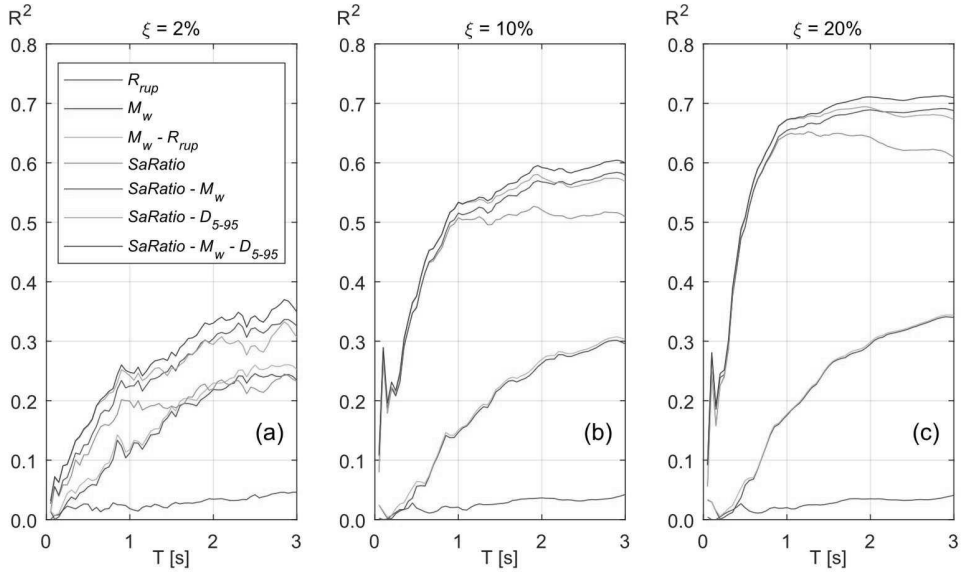

Figure 15. Coefficient of determination R^2 as a function of oscillator period for different regression models: a) 2% damping ratio; b) 10% damping ratio; and c) 20% damping ratio.

Figure 16 shows another relevant benefit of using *SaRatio* as a predictor for the damping modification factor η. Median η values as a function of *SaRatio* are plotted for the binned by magnitude ground motion dataset, using the same magnitude intervals of Figure 5, for damping levels $\xi = 1\%, 2\%, 3\%, 10\%, 20\%$, and 30%. For systems with damping levels higher than 2%, the η versus *SaRatio* relationship shows considerably less dependency on earthquake magnitudes than the η versus period of vibration relationship. Based on this fact, regression-based prediction expressions for η are considerably simpler and more robust if *SaRatio* is used

as a predictor, as their regression parameters will not depend on the magnitude range used for the statistical analysis. This means that most of the influence of magnitude on η is computed by considering *SaRatio* as a predictor.

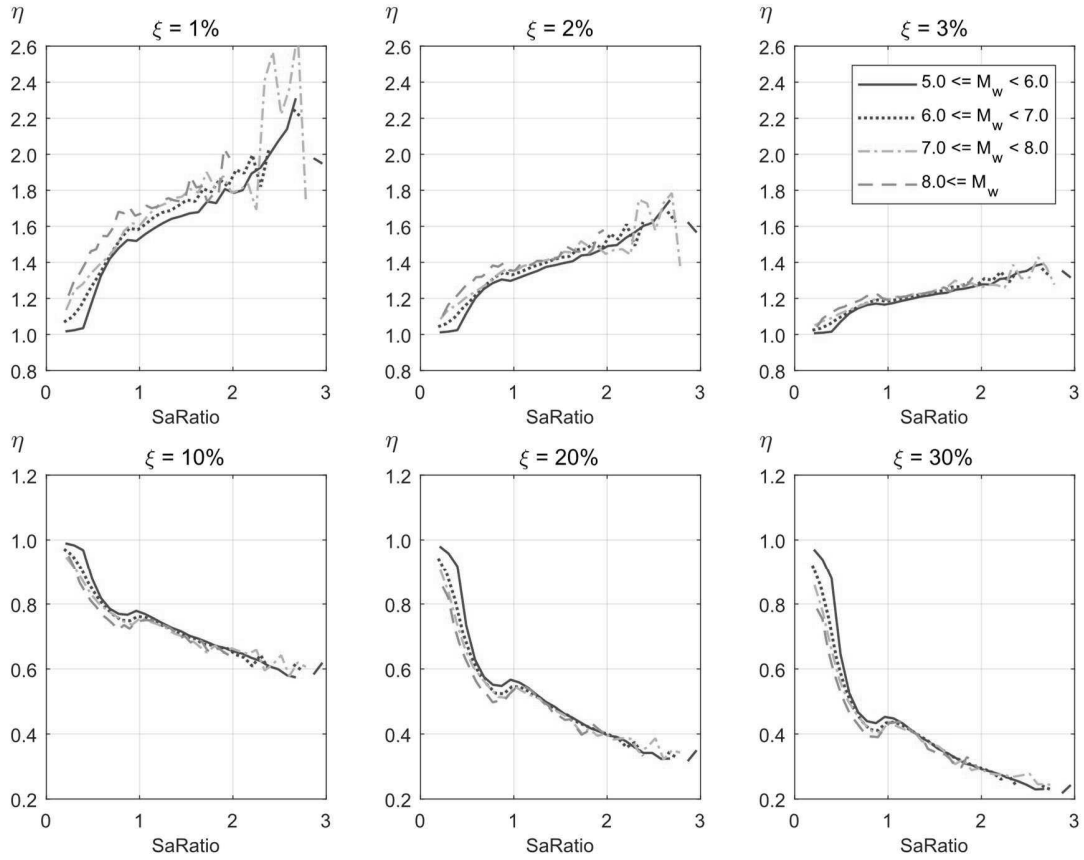

Figure 16. Median η values as a function of *SaRatio* for magnitude-binned ground motion records.

REGRESSION MODEL

Damping modification factor η is dependent on damping ratio and oscillator period, as it has been extensively documented in the literature and confirmed by results from this study. On the other hand, earthquake duration and/or event magnitude, are also known to influence η. However, based on the results of this study, their correlations are not as strong as the one with *SaRatio*, especially for systems with high damping. Additionally, as it can be seen in Figure 16, the η versus *SaRatio* relationship presents only a minor magnitude dependency for the complete *SaRatio* range and damping ratios above 2%.

Figure 17 shows scatter plots of η as a function of *SaRatio,* for systems with 10% and 20% critical damping and vibration periods T = 0.5 s, 1.5 s, and 3.0 s. As it can be seen in this

figure, the relationship between η and *SaRatio* is not strongly influenced by the oscillator period for which *SaRatio* is calculated. As the oscillator period shortens, the maximum value of *SaRatio* increases; however, the exponential trend between these two variables is similar, regardless of the oscillator period under consideration. Based on this fact, the variation of η as a function of *SaRatio* could be treated approximately as period independent, and a simplified model for evaluating η only as a function of *SaRatio* and ξ can be proposed.

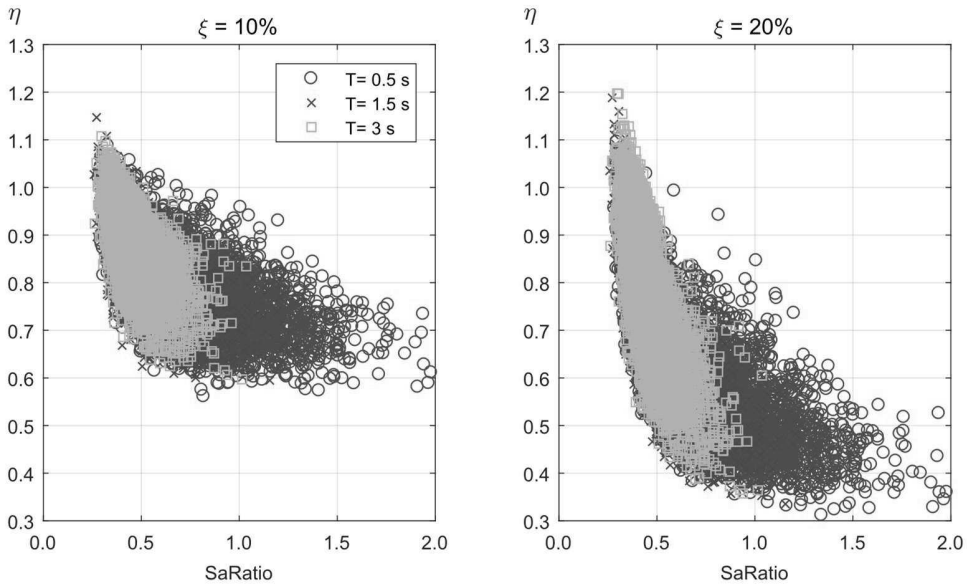

Figure 17. η versus *SaRatio* scattered data for different oscillator periods.

Figure 18 shows a tridimensional scatter plot of the three variables under study. On the horizontal plane, the axes are ξ and *SaRatio,* and the vertical axis is η. *SaRatio* and η values were calculated for six vibration periods T = 0.5 s, 1.0 s, 1.5 s, 2.0 s, 2.5 s, and 3.0 s for the complete ground motion set, resulting in a total of 31,620 points for each damping ratio. As the calculation was repeated for damping ratios of ξ = 10%, 12%, 15%, 18%, 20%, and 25%, the total number of (ξ, *SaRatio,* η) samples increases to 189,720

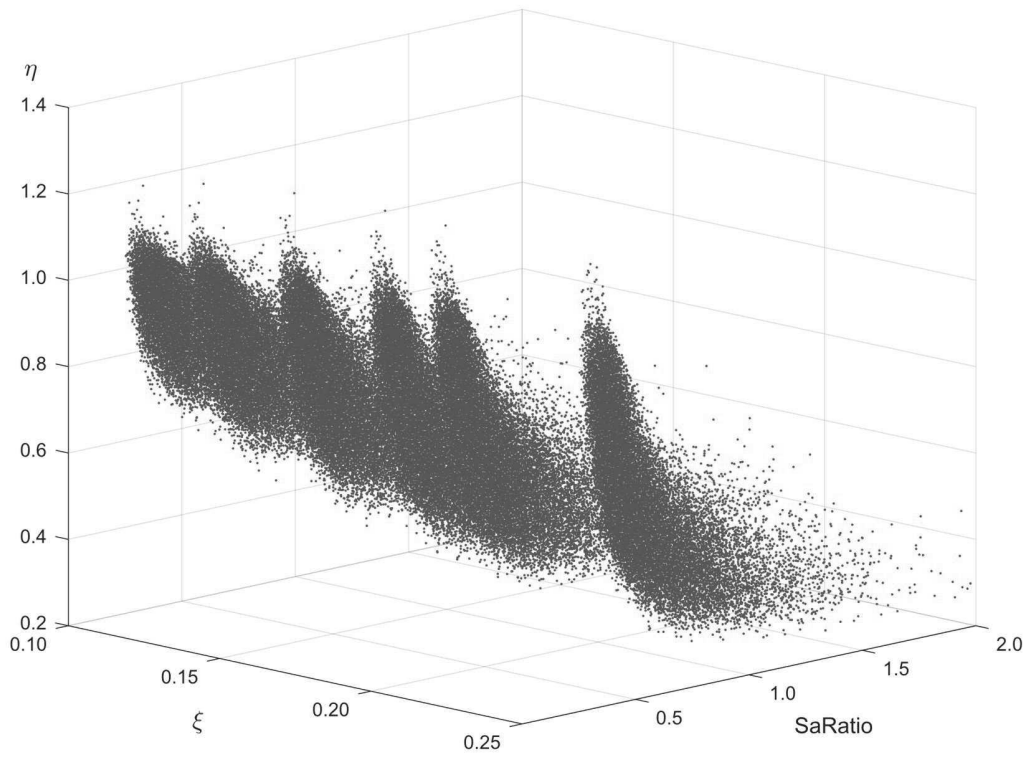

Figure 18. 189,720 (*ξ, SaRatio, η*) sample points to perform non-linear regression.

Several functional forms were studied to propose a sufficiently simple, but reasonably accurate, model. A functional form composed by the addition of two exponential terms is finally proposed:

$$\eta\,(\xi, SaRatio) = \exp\,(a_1 \cdot \xi) + \exp\,(a_2 \cdot SaRatio)$$

where coefficients a_1 and a_2 were determined through a nonlinear least square regression.

After performing the regression, the calculated values were $a_1 = -3.66$ and $a_2 = -3.22$. The proposed model is intended to be used with damping ratios between 0.10 and 0.25 and *SaRatio* values ranging from 0.40 to 1.60. The corresponding coefficient of determination R^2 over these ranges of *SaRatio* and damping ratios is 0.56. Figures 19 and 20 show a surface fitted through regression and plots of residual, respectively. Residuals are plotted as a function of *SaRatio* for different damping ratios.

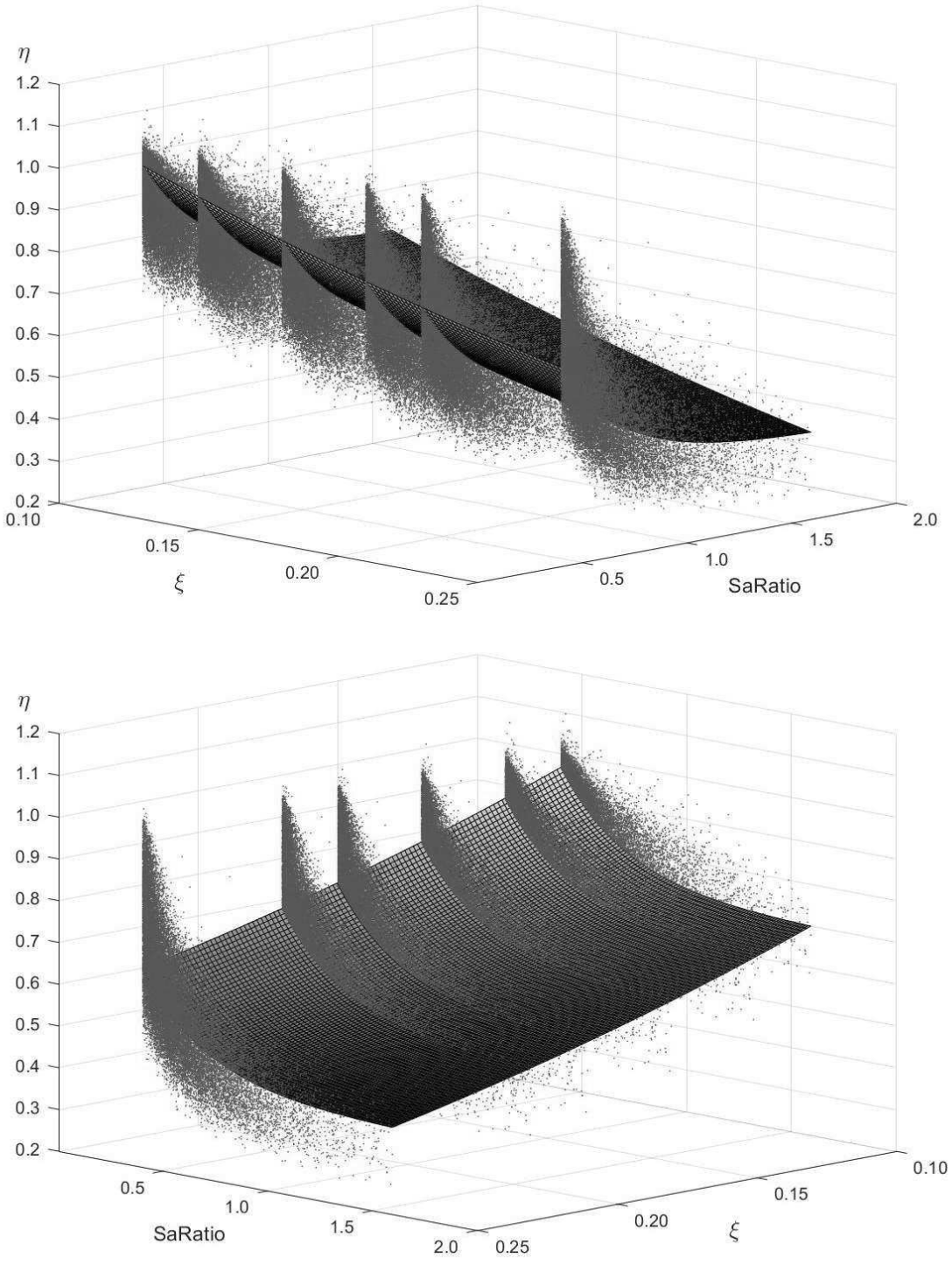

Figure 19. Proposed model to estimate η as a function of damping ratio ξ and *SaRatio* (same data, different views).

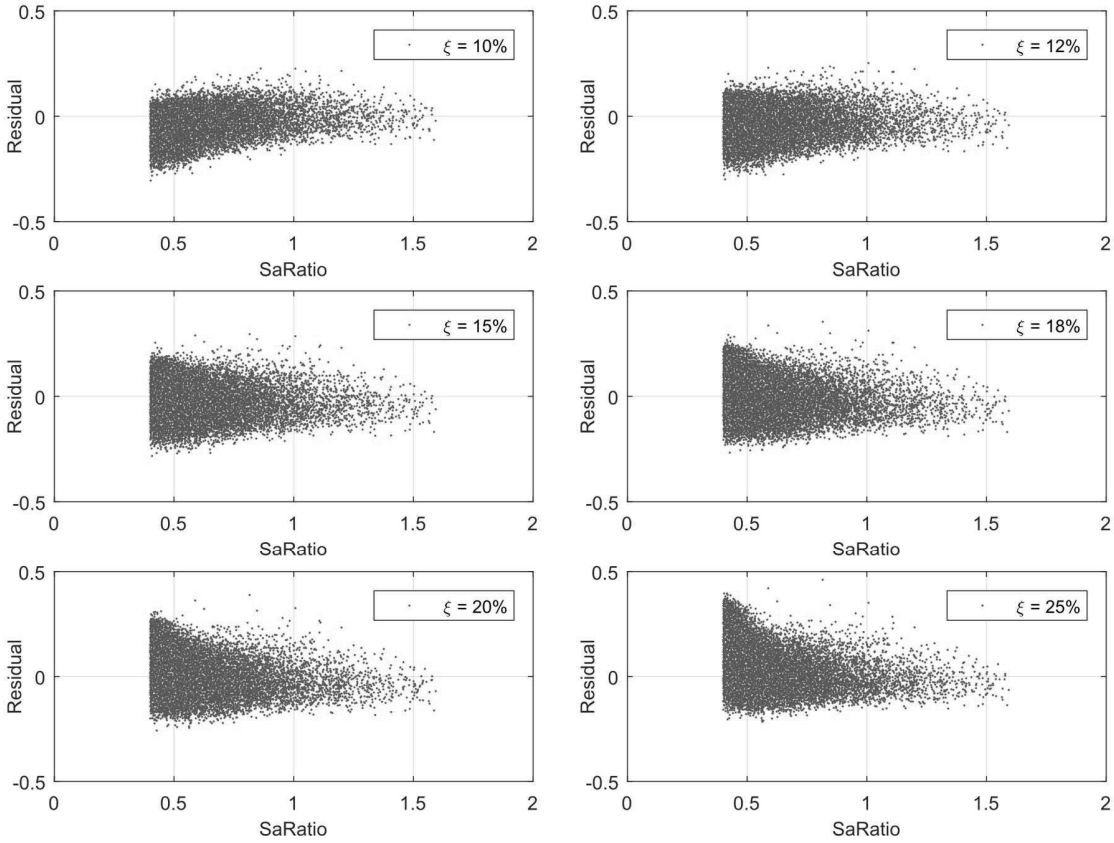

496

497 **Figure 20.** Residuals between observed and estimated damping modification factors η as a
498 function of ξ and *SaRatio*.

499 ## SUMMARY AND CONCLUSIONS

500 This study has presented a statistical analysis of damping modification factors η that permit
501 to estimate spectral ordinates corresponding to any value of damping ratio as a function of 5%
502 spectral ordinates. Damping modification factors were computed for a recently compiled
503 Chilean ground motion dataset that includes 5,270 ground motions recorded during 1,137
504 seismic events. Displacement modification factors were computed for oscillators with periods
505 of vibration ranging from T = 0.05 s to T = 6.0 s, and damping ratios ranging from 0.5% to
506 50%. These displacement modification factors were calculated considering arbitrary horizontal
507 components and RotI50 horizontal components, being the difference between these two
508 calculation approaches negligible. Results from statistical analysis are generally consistent
509 with widely used regression models from previous studies when the same magnitude bounds
510 are considered.

The novelty in this study is the evaluation of the effect of spectral shape on η, using two recently-proposed spectral shape proxy parameters as epsilon (ε) and *SaRatio*. A detailed analysis is presented to determine the optimal period range to be used for *SaRatio* calculation. Although strictly speaking optimal period range is period and damping dependent, reasonable results are obtained when a constant period range of $[0.2 \cdot T_1, 1.3 \cdot T_1]$ is used for calculating *SaRatio* to estimate the peak displacement response of systems with damping ratio different than 5%.

Results show that *SaRatio* is a better predictor than earthquake magnitude or than duration, especially in moderate and long-period systems, and in highly damped structures. On the other hand, epsilon (ε) does not show any significant statistical correlation with η.

In highly damped structures, the η versus *SaRatio* relationship was proven to be only mildly dependent on oscillator period and earthquake magnitude. Therefore, based on this interesting observation, a straightforward regression model is proposed, which enables to estimate η only based on two predictors: damping ratio and *SaRatio*.

Earthquake faulting mechanism was found not to have a significant influence on η when events with similar magnitudes and durations are compared. The effect of soil class was also studied, and its influence on η variability was also found to be negligible for site classes A, B C, and D.

A comparison between median η values from this statistical analysis and currently implemented B_D or B_M demand reduction values in Chilean code NCh 2745 was performed. Results show that η factors are strongly dependent on earthquake magnitude, an aspect that is currently neglected and could be introduced in future versions of the code. Larger magnitude earthquakes tend to show reductions that are, on average, 16% smaller than the reductions prescribed by the code, while smaller magnitude earthquakes lead to reductions significantly smaller than the ones predicted by the code.

ACKNOWLEDGMENTS

This research was funded by CONICYT Doctorado Nacional 21161027, the National Research Center for Integrated Natural Disaster Management CONICYT /FONDAP/15110017, and CONICYT/FONDECYT/1170836. We also thank the John A. Blume Earthquake Engineering Center at Stanford University. The seismic database used in

this work was provided by the project SIBER-RISK: Simulation Based Earthquake Risk and Resilience of Interdependent Systems and Networks CONICYT/FONDECYT/1170836.

ELECTRONIC SUPPLEMENT

Additional figures showing comparisons between various η predictors for different oscillator periods and damping ratios are available in the electronic supplement of this manuscript.

REFERENCES

Akkar, S., Sandıkkaya, M. A., and Ay, B. Ö., 2014. Compatible ground-motion prediction equations for damping scaling factors and vertical-to-horizontal spectral amplitude ratios for the broader Europe region. *Bulletin of earthquake engineering*, **12(1)**, 517-547.

American Society of Civil Engineers (ASCE), 2017. *Minimum Design Loads for Buildings and Other Structures*, *ASCE/SEI 7-16,* Reston, VA.

Baker, J.W., and Allin Cornell, C., 2006. Spectral shape, epsilon and record selection. *Earthquake Engineering & Structural Dynamics*, **35(9)**, 1077-1095.

Beyer, K., and Bommer, J. J., 2006. Relationships between median values and between aleatory variabilities for different definitions of the horizontal component of motion. *Bulletin of the Seismological Society of America*, **96(4A)**, 1512-1522.

Bommer, J.J., and Martinez-Pereira, A., 1999. The effective duration of earthquake strong motion. *Journal of earthquake engineering*, ***3*(02)**, 127-172.

Bommer, J.J., and Mendis, R., 2005. Scaling of spectral displacement ordinates with damping ratios, *Earthquake Engineering & Structural Dynamics*, **34(2)**, 145-165.

Boore, D. M., 2010. Orientation-independent, nongeometric-mean measures of seismic intensity from two horizontal components of motion. *Bulletin of the Seismological Society of America*, **100(4)**, 1830-1835.

Bozorgnia, Y., and Stewart, J.P. (Ed.), 2020. *Data Resources for NGA-Subduction Project*, *PEER Report 2020/02*. Pacific Earthquake Engineering Research Center, Berkeley, CA, 179pp.

Bradley, B.A., 2015. Period dependence of response spectrum damping modification factors due to source-and site-specific effects, *Earthquake Spectra*, **31(2)**, 745-759.

Cameron, W.I., and Green, R.A., 2007. Damping correction factors for horizontal ground-motion response spectra, *Bulletin of the Seismological Society of America*, **97(3)**, 934-960

Daneshvar, P., Bouaanani, N., Goda, K., and Atkinson, G.M., 2016. Damping reduction factors for crustal, inslab, and interface earthquakes characterizing seismic hazard in southwestern British Columbia, Canada. *Earthquake Spectra*, **32(1)**, 45-74.

Eads, L., Miranda, E. and Lignos, D., 2016. Spectral shape metrics and structural collapse potential, *Earthquake Engineering & Structural Dynamics*, **45(10)**, 1643-1659.

Hancock, J., Watson-Lamprey, J., Abrahamson, N. A., Bommer, J. J., Markatis, A., McCoy, E. M. M. A., & Mendis, R., 2006. An improved method of matching response spectra of recorded earthquake ground motion using wavelets. *Journal of earthquake engineering*, **10(spec01)**, 67-89.

Instituto Nacional de Normalización (INN), 2003. *Norma Chilena NCh2369 Oficial2003 Diseño sísmico de estructuras e instalaciones industriales*, Chile (in Spanish).

Instituto Nacional de Normalización (INN), 2013. *Norma Chilena NCh2745 Oficial2013 Análisis y Diseño de Edificios con Aislación Sísmica*, Chile (in Spanish).

Lin, Y.Y., and Chang, K.C., 2004. Effects of site classes on damping reduction factors, *Journal of Structural Engineering*, **130(11)**, 1667-1675.

Lin, Y.Y., Miranda, E., and Chang, K.C., 2005. Evaluation of damping reduction factors for estimating elastic response of structures with high damping, *Earthquake engineering & structural dynamics*, **34(11)**, 1427-1443.

Montalva, G. A., Bastías, N., & Rodriguez-Marek, A., 2017. Ground-motion prediction equation for the Chilean subduction zone. *Bulletin of the Seismological Society of America*, **107(2)**, 901-911.

Naeim, F., & Lew, M., 1995. On the use of design spectrum compatible time histories. *Earthquake Spectra*, **11(1)**, 111-127.

Newmark, N. M., and Hall, W. J., 1982. *Earthquake Spectra and Design*, Earthquake Engineering Research Institute, Oakland, CA.

Rathje, E. M., Faraj, F., Russell, S., and Bray, J. D., 2004. Empirical relationships for frequency content parameters of earthquake ground motions, *Earthquake Spectra*, **20**, 119-144.

Rezaeian, S., Bozorgnia, Y., Idriss, I.M., Campbell, K.W., Abrahamson, N., and Silva, W.J., 2012. *Spectral Damping Scaling Factors for Shallow Crustal Earthquakes in Active Tectonic Regions*, *PEER Report 2012/01*. Pacific Earthquake Engineering Research Center, Berkeley, CA, 168pp.

Simulation Based Earthquake Risk and Resilience of Interdependent Systems and Networks (SIBER-RISK), 2019. Web page for SIBER-RISK: Simulation Based Earthquake Risk and Resilience of Interdependent Systems and Networks CONICYT/FONDECYT/1170836 Strong Motion Database, available at https://siberrisk.ing.puc.cl/StrongMotionDatabase (last accessed October 30, 2019)

603 Stafford, P.J., Mendis, R. and Bommer, J.J., 2008. Dependence of damping correction factors for
604 response spectra on duration and numbers of cycles, *Journal of Structural Engineering*, **134(8)**,
605 1364-1373.